Journal of Ceramic Processing Research. Vol. 13, Special. 2, pp. s422~s427 (2012)

J O U R N A L O F
Ceramic Processing Research

Aging effect analysis of long period operating composite insulators in different electric field position

Yun-Peng Liu*, Xiao-Hui Yang, Ying Liang and Rui-Feng Zhang
Hebei Provincial Key Laboratory of Power Transmission Equipment Security Defense, North China Electric Power University, Baoding, China

Electric field distribution is one of the important factors which impact the aging of composite insulators. The electric field of composite insulators was simulated by ANSYS software, and the shed samples in different parts of the composite insulator were analyzed by Fourier transform infrared spectroscopy (FTIR). The characteristic peaks of functional groups in the main chain and side chain of composite insulator material molecular formula were compared. The smaller the characteristic peak area is, the less the corresponding functional group is, that means the facture condition of main chain or side chain is more serious. In this way, the characteristic peaks of samples in different electric field distribution were compared, and the influence of electric field distribution to the aging effect of the composite insulators is gained. The results show that electric field strength is the strongest in the composite insulator high-voltage side, followed by low-voltage side, and the electric field in the middle of the composite insulator is the lowest. Accordingly, the aging degree in the composite insulator high-voltage side is the most serious, followed by low-voltage side, and the aging degree is weakest in the middle part.

Keywords: Aging, Composite insulators, Electric field, Fourier transform infrared spectroscopy (FTIR).

Introduction

Recently, composite insulators have been used more and more widely around the world, due to their unique hydrophobicity, lightweight structure and easy installation, especially in medium and heavy polluted region. Over 4 million composite insulators are used in transmission lines in China [1-3]. After long-term running in the harsh environments of sun exposure, acid rain, high field strength, and so on, composite insulators can be aging, for the inherent nature of composite materials. These environmental factors all affect aging. Domestic and foreign scholars have done a lot of artificial accelerated aging research: full-wavelength UV accelerated aging test, fixed-wavelength UV accelerated aging test, and DC or AC corona accelerate aging test [4-6]. But these tests are very different of actual operating conditions. The accurate aging model of composite insulators has not been established until now.

The aging is complex physical and chemical phenomena, with the physical parameters (hardness, hydrophobicity, etc.) and chemical parameters (surface element contents, molecular bond fracture degree, oxidation products, etc.) of composite insulators changing in the aging process. There will be certain research methods, corresponding to a certain amount of physical or chemical parameters. X-ray photoelectron spectroscopy (XPS) can be used to quantitatively measure composite insulator surface element contents; scanning electron microscopy (SEM) can be used to directly observe the large particles, pollution, empty, cracks and surface roughness of composite insulator surface; Fourier transform infrared spectroscopy (FTIR) can be used for analyzing the molecular structure [7-10]. Composite insulators are mostly composed of silicone rubber materials, the composition of which is relatively simple, but different manufacture has different amount of additives. This paper mainly considers the molecular microcosmic structure change in the aging process. Different parts of a insulator are analyzed with the attenuated total internal reflectance (ATR)-FTIR method, to get the effect of electric field to aging.

*Corresponding author:
Tel : +86-312-7522385
Fax: +86-312-7522252
E-mail: gylyp@263.net

Principle and Method

Principle of ATR-FTIR

When a beam ,which has a continuous wavelength of infrared light, pass through a material, if the rotational frequency or the vibration frequency of a certain chemical groups in the molecule is same as infrared light frequency, the molecules will absorb energy, and transit from the ground state vibrational (rotational) level to higher vibrational (rotational) energy level. Then the frequency (wavelength) of the infrared light will be absorbed by the material. Therefore, infrared spectroscopy is essentially an analysis method, based on relative molecular vibration and molecular rotation to determine the

substance's molecular structure.

ATR-FTIR technique is a method of infrared analysis, which could be applied to measure directly with no treatment of the material surface. The samples are closely attached to the total reflection prism. If the incident angle is greater than the critical angle, when it goes a certain depth into the optical sparse medium (sample), the incident light will retrace to the total reflection prism. Because of the effect of the standing wave, some wavelength infrared lights can be absorbed by the sample to be attenuated, with different Attenuation degree of certain wavelength infrared light related to the sample structure. The principle of ATR is shown in Fig. 1. The following section is a total reflection prism, and the top section is the insulator sample. The light path is shown in the figure, with standing wave forming on the sample bottom surface. The amplitude of the standing wave has a sharp attenuation in space. The penetration depth of standing wave is micron level, in this sense, ATR-FTIR reflects the sample surface state information.

Analysis methods of infrared spectroscopy

A typical infrared spectrum of the sliced silicone rubber insulator, which is manufactured by a Chinese company, is shown in Fig. 2. The wave number, which is the reciprocal of the wavelength, is used as abscissa, so different wave number corresponds to specific wavelength of infrared light. The transmittance is used as ordinate, and the lower the transmittance is the more the specific wave number infrared light is absorbed. The formula of silicone rubber formula is relatively simple, its main chain is made by Si-O-Si, and the

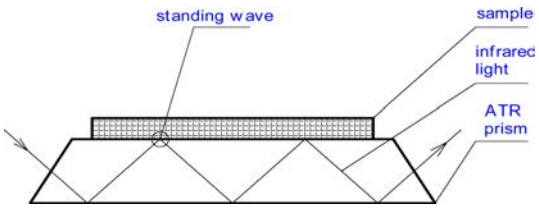

Fig. 1. Principle of ATR.

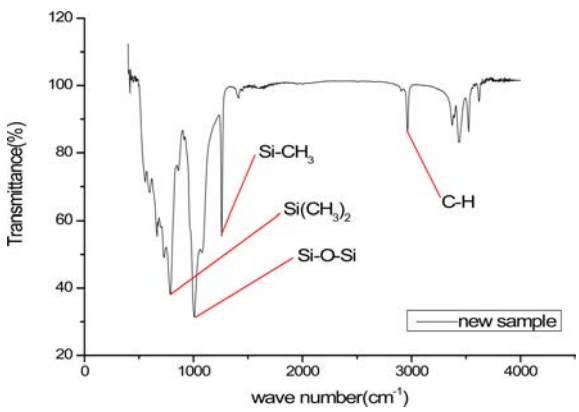

Fig. 2. Infrared spectrum of new sample.

Table 1. Wave Number of Chemical Group Characteristic Peak.

chemical group	wave number of characteristic peak
$Si\text{-}CH_3$	1,270 cm^{-1}
$Si(CH_3)_2$	800 cm^{-1}
C-H	3,000 cm^{-1}
Si-O-Si	1,000-1,100 cm^{-1}

$Si(CH_3)_2$ forms its side chain. From Fig. 2, it is evident that there are absorption peaks at the wave number of chemical groups, which are listed in Table 1. There are also absorption peaks at the wave number from 3,400 to 3,700 cm^{-1}, which correspond to the hydroxyl (OH band). In order to improve the flame retardancy of insulator materials, materials will be added $Al(OH)_3$, while at the same time, OH is also a product of aging, so it is not a suitable band to analyze [11].

There are two ways for FTIR quantitative analysis, one is to measure the height of the peak of absorption wave, and the other way is to measure the area of the absorption peak. The two methods have a similar principle. The more of the chemical group is, the more of infrared light is absorbed, and the smaller of the transmittance is, the larger of the height and area of the absorption peak. Whether the height method or the area method is applied, a base line must be established first. There are two ways of baseline selection, one is selecting a same baseline in the IR spectrum, and the absorption peak values or area values are relative to this baseline value; the other is connecting the two ends of the absorption peak as a baseline. Peak area, which is more precise than peak height to conduct the quantitative analysis, is selected to analyze the silicone rubber material, and the connecting line of the two ends of the absorption peak is selected as a baseline. A same baseline is selected to analyze a chemical group, so the two highest points of the two ends of the absorption peak are connected as the base line, from the two ends of which, the verticals are drawn to form the peak area with baseline and the absorption peak. The baseline and the area of characteristic peaks of main chain are shown in Fig. 3 [12].

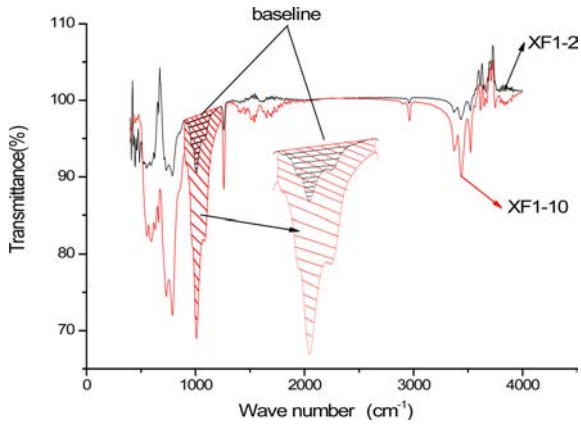

Fig. 3. Baseline and area of Si-O-Si.

Results and Discussion

Establish of the simulation models of composite insulators

First, the finite element model in ANSYS was established according to the actual parameters of the composite insulators, which had been operating for 19 years, and the electric field in the vicinity of the composite insulators at the operating voltage is calculated. Structure parameters of composite insulators used in this article are: structure height H = 1220 mm, insulation length h = 980 mm, rod diameter is 32 mm, sheds number is 19, shed diameter = 117 mm, and umbrella spacing = 48 mm. There are several assumptions in the paper: first, composite insulator surface is clean and dry; second, the Towers and the conductors have a smaller impact than the grading ring to the electric field strength, and the impact area is limited. Therefore the impact of the conductor and tower are ignored in the calculation process, with a radius of 20 cm disc to simulate the impact of the cross arm, and the whole model can be simplified to an axisymmetric two-dimensional electric field analysis model. According to the calculation experience, the selected finite elements are unit Plane121, and far-field unit INFIN110; the relative dielectric constant of the air and the silicone rubber are respectively 1 and 4; the voltage of high-voltage end is the operating voltage, 110 kV; while in order to improve accuracy, fine subdivision area are set near the silicone rubber, fittings and sheath. Fig. 4 shows the insulator model, which is only half of the insulator due to symmetry.

The simulation results

Fig. 5 is the electric field distribution curve at the axial distance of 78 mm from the insulator. The origin of the curve is selected near the second sheds of high-voltage end. The maximum electric field strength is there with the grading ring. It is evident that the electric field strength is the strongest in the composite insulator high-voltage side, followed by low-voltage side, and the electric field in the middle of the composite insulator is the lowest. And the strongest electric field strength is nearly 8 times of the lowest field.

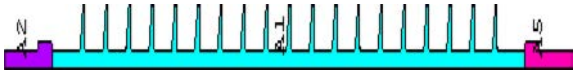

Fig. 4. Composite insulators model.

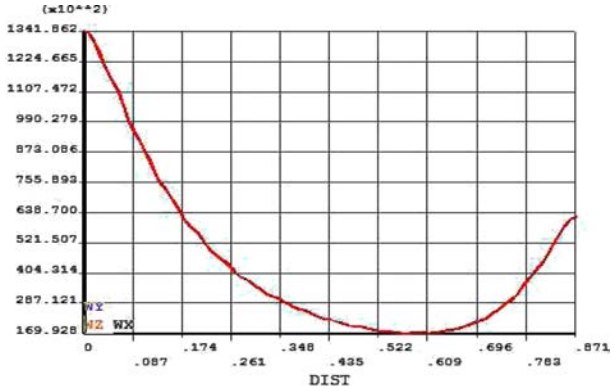

Fig. 5. Electric field curve.

Infrared spectrum test results

The shed samples (r = 1 cm, h = 0.1 cm) in different parts of the insulator were cut, and analyzed by FTIR to obtain the infrared spectra of the samples. The samples were taken from three-phase insulator of 110 kV. The insulators, 19 sheds, were produced by a Chinese manufacturer. The sheds are numbered from the high-voltage end, and the sheds in different position of the insulators are shown in Table 2.

Test infrared spectrums results of top surface

The top surface infrared spectrums of XF1, XF2 and XF3 are shown in Figs. 6-8. Si-O-Si and Si-$(CH_3)_2$ infrared spectrums of XF1 are shown in Fig. 9, in order to clearly show the peak sixe.Compared with Fig. 2, it is evident that, due to the effects of aging the polymeric groups corresponding to characteristic peaks have been reduced. Sheds in different parts is not a same aging degree: the sheds of high-voltage end and low-voltage end have a stronger aging than the middle sheds.

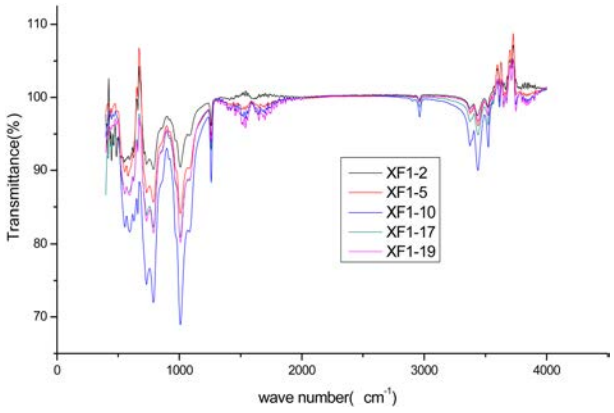

Fig. 6. Top surface infrared spectrums of XF1.

Table 2. Sample Information.

Insulator numbers	Running voltage	Tower number	Phase	Run years	Sheds number
XF1		17#	left		2-5-10-17-19
XF2	110 kV	17#	middle	19	5-9-11-17-19
XF3		17#	right		3-11-16

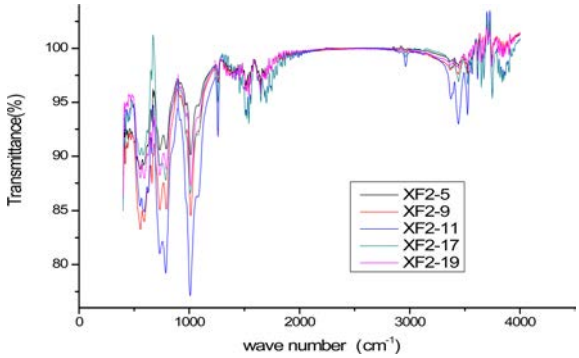

Fig. 7. Top surface infrared spectrums of XF2.

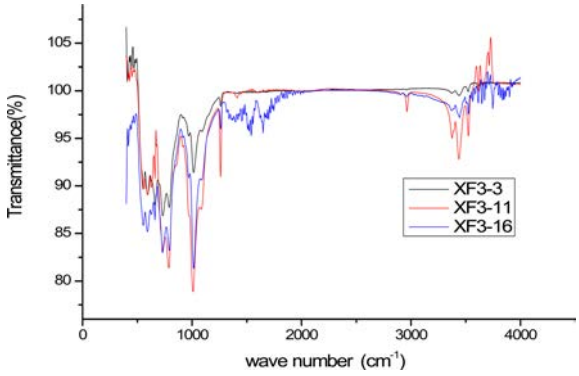

Fig. 8. Top surface infrared spectrums of XF3.

The aging of the shed is analyzed through the analysis way of the peak area. The infrared spectrumof the most serious aging shed has a smallest absorbed peak area, which corresponds to the strongest electric field. So the area is normalized in this way: First, the max area of characteristic peaks of different sheds (MAXA) is found, and set to 1; relative area values of other sheds characteristic peaks (relative valve) are the ratio of the max area and their actual value. The formula is as follows:

$$\text{Relative value} = \text{MAXA}/\text{AREA} \quad (1)$$

At last, the relative values of same phase insulator are all multiplied by an adjustment factor, and then normalized values are gained. This value is defined as aging index. The higher value indicates less chemical group content, more serious molecular bond fracture, and thus more serious aging.

Relationship between main chain aging index and electric filed

The wave number of the characteristic peak of Si-O-Si bond in the main chain is 1,000-1,100 cm^{-1}, the scatters are plot by the aging index values of absorb peak of Si-O-Si bond in main chain of XF1-XF3. The relative values curve of electric field is plot in the same figure to compare the electric field and the aging degree. As shown in Fig. 10, the dist is as the abscissa,

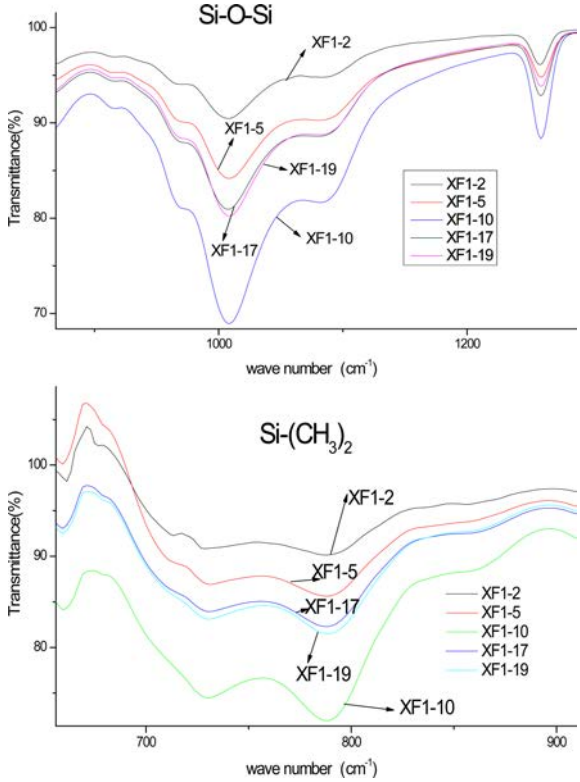

Fig. 9. Si-O-Si and Si-$(CH_3)_2$ infrared spectrums of XF1.

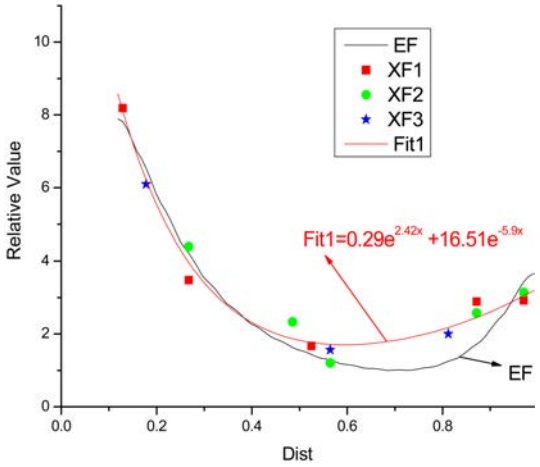

Fig. 10. Main chain (Si-O-Si).

which indicates the distance from high-voltage end to low-voltage end (from the second shed to the 19th shed). The aging index value and the relative field value are as the ordinate.

Taking into account the aging index of XF1, XF2 and XF3, the aging index of the same number shed of different insulator are averaged, and they are fitted by double exponential function. Fig. 10 shows the results of double exponential fitting, fitting curve $Fit1 = 0.29e^{2.42x} + 16.51^{-5.9x}$, $Fit11 = 0.29e^{242x}$ is an increasing function, corresponds to the increase of the aging intensified at the low voltage side, $Fit12 = 16.51e^{-5.9x}$ is a decreasing function, corresponding to the aging

intensity decrease at the high voltage side. Fig. 10 obviously shows that the fitted curve and the electric field curve have a similar trend. The 89 Interpolated data of electric field curve and fitting curve have a correlation coefficient of 0.9788.

Infrared spectrum is an effectively way to analyze the molecular chain fracture, and corona discharge is an important factor to cause the silicone rubber material aging. The local surface aging of composite insulator sheds and sheath, too strong field of end side, caused by unreasonable designing of the grading ring, the failure of internal insulation, surface contamination, surface wetting and many other factors will make the surface of the operating voltage composite insulator possible in a long-term corona discharge. Obviously, the intensity of the corona discharge is closely related with the electric field strength.

The bond energy of Si-O, Si-C, and C-H in the methyl are respectively 446 kJ/mol, 301 kJ/mol and 413 kJ/mol. Based on the electric field and the mean free path of the air in the process of corona discharge, the charged particles, which are excited by corona discharge, have enough energy to damage the molecular structure of silicone rubber material. Corona discharge generated high-energy electron beams and ion beams, which would hit silicone rubber surface. The high temperature and mechanical collision can split Si-O-Si bond two free radicals, CH_3 and H. Meanwhile corona discharge will produce a lot of ozone, a highly active strong oxidant, which can oxidize unsaturated Si-O-Si bond from the cracking reaction at high temperature. H hatoms in the lateral methyl or methylene can easily be replaced by the hydroxy (OH) to form silanol [6]. The chemical reaction is shown in Fig. 12.

Relationship between side chain aging degree and electric field

There are $Si(CH_3)_2$ bond, $Si\text{-}CH_3$ bond and C–H bonds in side chain. The characteristic peak areas of $Si\text{-}CH_3$ bond and C-H bond are very small, which is interfered by measuring conditions, therfore only the Si

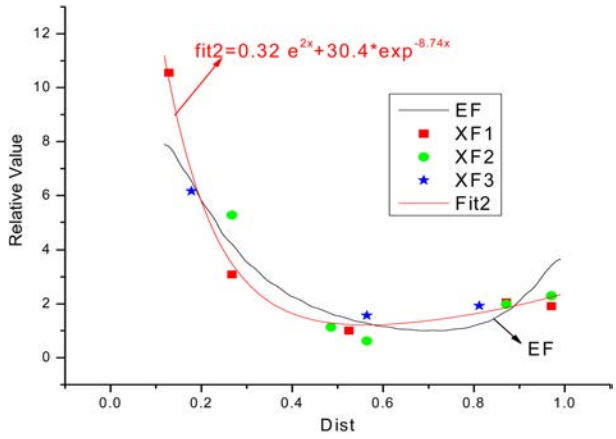

Fig. 11. Side chain ($Si(CH_3)_2$).

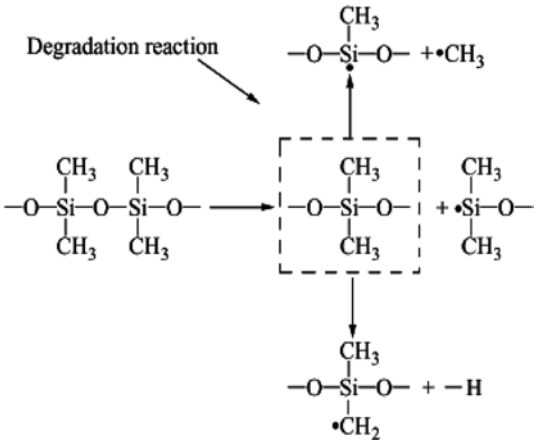

Fig. 12. Chemical reaction.

$(CH_3)_2$ bond is analyzed, as shown in Fig. 11. The curve in Fig. 11 have the same trend as in Fig. 10, indicating that the fracture simultaneously occur in main chain and side chain. Like the previous analysis, double exponential fitting curve is

$$Fit2 = 0.32e^{2x} + 30.4e^{-8.74x} \quad (2)$$

And the correlation coefficient is 0.9463. This correlation coefficient is less than the correlation coefficient of the main chain, and the aging curve and the field curve of main chain have a more higher similarity.

Conclusion

The results can be used as a reference of the influence of the electric field to the composite insulator aging effects, and can provide theoretical and experimental basis for that Fourier transform infrared spectroscopy can be a one of the basis for judging aging effect. Nevertheless, the results of the study was got based on some samples. The further promotion of the result needs to collect more samples to conduct a systematic study.

Acknowledgements

This work was supported by the National Basic Research Program of China (973 Program) (2011CB209401), National Science Foundation of China (912011208) and Fok Ying Tong Education Foundation (121058).

References

1. F. Zhao, F.Z. Zhang, H.L. Yang, Z.C. Guan, L.M. Wang, H. Wen and Y. Ma, Proceedings of the CSEE 29 [1] (2009) 58.
2. CIGRE Working Group 22-03, Electra 130 (1990) 58.
3. R. Hackam, IEEE Transactions on Dielectrics and Electrical Insulation 6 [5](1999) 557.
4. X.D. Liang, Z.. Li, Y.X. Zhou, Proceedings of the CSEE 27 [27] (2007) 19.

5. L. Lan, X.S. Wen and H. Liu, High Voltage Engineering 35 [35] (2009) 2652.
6. J.G. Wang, Y. Liu, C.H. Fang, J.J. Chen, C.Z. Xie, and L. Cai, Acta Polymerica Sinica 4 (2009) 331.
7. J.P. Habas, J.M. Arrouy and F. Perrot, IEEE Transactions on Dielectrics and Electrical Insulation 16 [5] (2009) 1444.
8. S. M. Rowland, J. Robertson, Y. Xiong and R. J. Day, IEEE Transactions on Dielectrics and Electrical Insulation 17 [2](2010) 375-383.
9. P.D. Blackmore, D. Birtwhistle, G.A. Cash and G.A. George, IEEE Transactions on Dielectrics and Electrical Insulation 5 [1] (1998) 132.
10. G. Cash, G. George, P. Blackmore and D. Birtwhistle, in Proceedings of Seventh International Conference on Dielectric Materials Measurements & Application, September (1996) 285.
11. S. Kumagai and N. Yoshimura, IEEE Transactions on Dielectrics and Electrical Insulation 8 (2001) 203.
12. C.Z. Xie, Y. Zhang, J.G. Wang, Y.P. Hao, M.Z. Gao and Y. Liu, in Proceedings of the 9th International Conference on Properties and Applications of Dielectric Materials, July (2009) 321.